Hindawi Publishing Corporation
Evidence-Based Complementary and Alternative Medicine
Volume 2014, Article ID 247595, 12 pages
http://dx.doi.org/10.1155/2014/247595

Research Article

The Spectroscopy Study of the Binding of an Active Ingredient of *Dioscorea* Species with Bovine Serum Albumin with or without Co^{2+} or Zn^{2+}

He-Dong Bian,[1,2] Xia-Lian Peng,[2] Fu-Ping Huang,[2] Di Yao,[2] Qing Yu,[2] and Hong Liang[2]

[1] *Key Laboratory of Development and Application of Forest Chemicals of Guangxi, Guangxi University of Nationalities, Nanning 530006, China*
[2] *Key Laboratory for the Chemistry and Molecular Engineering of Medicinal Resources (Ministry of Education of China), School of Chemistry and Pharmaceutical Sciences of Guangxi Normal University, Guilin 541004, China*

Correspondence should be addressed to He-Dong Bian; gxunchem@163.com and Hong Liang; gxnuchem312@aliyun.com

Received 30 March 2014; Revised 6 May 2014; Accepted 15 May 2014; Published 4 June 2014

Academic Editor: Shi-Biao Wu

Diosgenin (DIO) is the active ingredient of *Dioscorea* species. The interaction of DIO with bovine serum albumin (BSA) was investigated through spectroscopic methods under simulated physiological conditions. The fluorescence quenching data revealed that the binding of DIO to BSA without or with Co^{2+} or Zn^{2+} was a static quenching process. The presence of Co^{2+} or Zn^{2+} both increased the static quenching constants K_{SV} and the binding affinity for the BSA-DIO system. In the sight of the competitive experiment and the negative values of ΔH^0 and ΔS^0, DIO bound to site I of BSA mainly through the hydrogen bond and Van der Waals' force. In addition, the conformational changes of BSA were studied by Raman spectra, which revealed that the secondary structure of BSA and microenvironment of the aromatic residues were changed by DIO. The Raman spectra analysis indicated that the changes of conformations, disulfide bridges, and the microenvironment of Tyr, Trp residues of BSA induced by DIO with Co^{2+} or Zn^{2+} were different from that without Co^{2+} or Zn^{2+}.

1. Introduction

Dioscoreaceae mainly distributes Guangdong, Sichuan, and Zhejiang provinces in China. Diosgenin (DIO), 3β-hydroxy-5-spirostene (Figure 1), one of the active ingredients of *Dioscorea* species, is derived from the tubers of *Dioscorea* species. The previous studies have indicated that DIO can retard the progression of osteoporosis [1] and attenuate plasma cholesterol [2], possess anti-inflammatory [3] and inhibition of vasoconstriction [4] effects, and so on.

Serum albumin (SA) is composed of three structurally homologous domains (I–III); each domain contains two subdomains (A and B). It is the major transport protein, which can act as a carrier of endogenous and exogenous ligands [5]. The transportation and distribution of the drugs in vivo are related to their interaction with serum albumin. On the other hand, the binding of drugs also can change the conformation function of serum albumin. So it is important to investigate the interaction between drugs and serum albumin. Bovine serum albumin (BSA) has similar structure and property with human serum albumin (HSA); the major difference between these two serum albumins was that there was only one Trp residue in HSA, but in BSA there were two Trp residues (^{134}Trp and ^{212}Trp). Compared with HSA, BSA was always selected as a model protein due to its low cost, unusual ligand-binding properties. The study of the interaction between drugs and BSA plays an important role in pharmacology and pharmacodynamics [6].

Blood plasma contains many metal ions which play important roles in the biochemical processes. The previous reports of interactions between serum albumin and several metal ions suggested that many metal ions have special binding sites on proteins [7–9]. The binding of drugs with serum albumin in the presence of metal ions was also extensively studied [10, 11]. The previous studies indicated that the presence of metal ions would not only affect the interaction

of serum albumin with drugs, but also the conformational changes of serum albumin induced by drugs. The metal ions of Co^{2+} and Zn^{2+} are abundant essential elements in organism which possess many biochemical functions. It is necessary to investigate the interaction of BSA-DIO in the presence of Co^{2+} or Zn^{2+}.

In this paper, we studied the binding of DIO with BSA under simulated physiological conditions of pH = 7.43. Fluorescence spectra and Raman spectra were employed to investigate the binding process and the changes of protein structure in the absence and presence of Co^{2+} or Zn^{2+}.

2. Materials and Methods

2.1. Materials. DIO (98%, purchased from Aladdin Reagent Company) was dissolved in ethanol to prepare a stock solution of 1×10^{-3} mol·L^{-1}. 0.05 mol·L^{-1} phosphate buffer solution (PBS) of pH = 7.43, contained 0.1 mol·L^{-1} NaCl. BSA (98%, fatty acid free, and globulin free, Sigma) was dissolved in PBS to prepare stock solution of 1×10^{-3} mol·L^{-1} and stored at 277 K, diluted before used. Ibuprofen and ketoprofen were dissolved in ethanol to prepare stock solution of 1×10^{-3} mol·L^{-1}, respectively. Sodium chloride, ethanol, zinc chloride, cobalt(II) chloride hexahydrate, and other experimental drugs are analytically pure reagents. Double distilled water was used throughout.

2.2. Fluorescence Spectrum. Fluorescence spectra were carried out on a RF-5301 fluorescence spectrophotometer (Japan Shimadzu Company). A solution of 5.0×10^{-7} mol·L^{-1} BSA was added in a 1.0 cm quartz cell; metal ions or DIO were then gradually added into BSA by microinjector. Scan the solution of BSA in the absence and presence of DIO or metal ions in the wavelength range of 300–500 nm, respectively. The slit widths were 5 nm/5 nm; the excitation wavelength was 280 nm. The reaction temperatures for DIO-BSA system without metal ions were controlled at 291 K, 298 K, and 306 K, respectively. The reaction temperatures for DIO-BSA system with Co^{2+} or Zn^{2+} were controlled at 298 K. For site marker experiment, BSA and site markers were mixed in equimolar concentrations at room temperature for 2 h, and then DIO was gradually added into the solution, scan the fluorescence spectra of the solution.

2.2.1. The Quenching Mechanism. In order to confirm the quenching mechanism induced by DIO, the fluorescence quenching was described by Stern-Volmer equation [12]:

$$\frac{F_0}{F} = 1 + k_q \tau_0 [Q] = 1 + K_{SV} [Q], \quad (1)$$

where F_0 and F are the fluorescence intensity in the absence and presence of quencher, respectively. k_q is the quenching rate constant. τ_0 is the average fluorescence lifetime of the biomolecule in the absence of quencher. $[Q]$ is the concentration of quencher. K_{SV} is the Stern-Volmer quenching constant. Since the fluorescence lifetime of the biopolymer is 10^{-8} s [13], K_{SV} and k_q can be obtained according to the slopes of the Stern-Volmer plots.

2.2.2. The Quenching Mechanism and the Binding Constant. The binding constants of the static quenching were calculated according to the modified Stern-Volmer equation [14]:

$$\frac{F_0}{(F_0 - F)} = \frac{1}{f} + \frac{1}{(Kf[Q])}, \quad (2)$$

where f is the fraction of accessible fluorescence and K is the effective quenching constant for the accessible fluorophores, which are analogous to associative binding constants.

2.2.3. Thermodynamic Parameters. The enthalpy change (ΔH^0) was regarded as a constant when the temperature changed little, then enthalpy change (ΔH^0) and entropy change (ΔS^0) can be obtained from Van't Hoff equation [15]:

$$\ln K = -\frac{\Delta H^0}{RT} + \frac{\Delta S^0}{R}, \quad (3)$$

$$\Delta G^0 = \Delta H^0 - T\Delta S^0 = -RT \ln K, \quad (4)$$

where R was the gas constant and ΔG^0 was the standard free energy change.

2.2.4. Energy Transfer Calculation. According to Forster's nonradiative energy transfer theory [16, 17], the energy transfer efficiency is decided not only by the distance between the acceptor and donor, but also the critical energy transfer distance (R_0); that is [18],

$$E = 1 - \frac{F}{F_0} = \frac{R_0^6}{R_0^6 + r^6}, \quad (5)$$

where r is the distance between acceptor and donor and R_0 is the critical distance in the case of the transfer efficiency is 50%

$$R_0^6 = 8.8 \times 10^{-25} K^2 n^{-4} \Phi J, \quad (6)$$

where K^2 is the spatial orientation factor of the dipole, n is the refractive index of the medium, Φ is the fluorescence quantum yield of donor, and J is the overlap integral of fluorescence emission spectrum of donor and absorption spectrum of acceptor

$$J = \frac{\sum F(\lambda) \varepsilon(\lambda) \lambda^4 \Delta\lambda}{\sum F(\lambda) \Delta\lambda}, \quad (7)$$

where $F(\lambda)$ is the fluorescence intensity of the donor at wavelength λ and $\varepsilon(\lambda)$ is the molar absorption coefficient of the acceptor at wavelength λ.

2.3. Raman Spectrum. The Raman spectra were recorded on a Renishaw Invia+Plus FT-Raman spectrometer using an Ar^+ laser with excitation wavelength of 514 nm. The laser power was 3 mW; the recording range was 200–2000 cm^{-1} with spectral resolution of 1 cm^{-1}. Scan the Raman spectra of 5×10^{-4} mol·L^{-1} BSA in the absence and presence of DIO and metal ions of the same concentration under the room

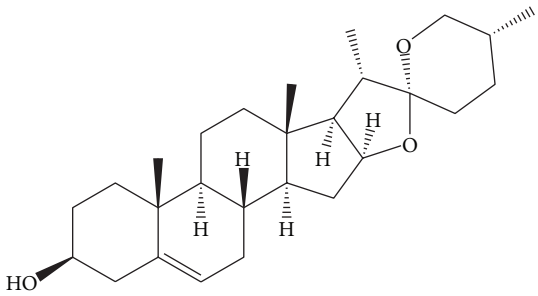

Figure 1: The chemical structure of diosgenin.

temperature. In Raman experiment, DIO was first dissolved in ethanol/water (1 : 9) and then mixed with BSA, metal ions solution to prepare Raman scanning sample. The curve fitting of Raman spectral regions was analysed by the curve-fitting procedure (Peak Analyzer module of Origin 8.0, Microcal Origin, USA) using Gaussian curves.

3. Results and Discussion

3.1. The Influence of DIO on the Fluorescence of BSA without or with Co^{2+} or Zn^{2+}. For macromolecules, the fluorescence measurements can give information of the binding of small molecule substances to protein. When excited at 280 nm, the intrinsic fluorescence of BSA was mainly contributed by Trp residues [19, 20]. The fluorescence of BSA quenched by DIO in the presence and absence of Co^{2+} or Zn^{2+} of the same concentration was shown in Figure 2. Figure 2(a) showed that the fluorescence intensity of BSA decreased regularly with increasing DIO. Meanwhile, the small blue shift observed with increasing DIO concentration indicated a more hydrophobic environment of the fluorescence chromophore of BSA [21]. Figures 2(b) and 2(c) showed that the fluorescence intensity decreased after adding Co^{2+} or Zn^{2+} with the same concentration. These indicated that the metal ions bind with BSA which is in accordance with our previous work. When DIO was added into BSA solution containing equimolar Co^{2+} or Zn^{2+}, the fluorescence intensity decreased regularly with blue shift. The shapes of spectra were similar to those in the absence of Co^{2+} or Zn^{2+}, while the fluorescence intensity in the presence of Co^{2+} or Zn^{2+} was weaker than those without Co^{2+} or Zn^{2+}. The result obtained suggested that the fluorescence was quenched not only by the metal ions but also by DIO. The interaction occurred among BSA, DIO, and the metal ions.

3.2. The Quenching Mechanism and the Binding Constant. Fluorescence quenching is classified as dynamic quenching and static quenching. Usually, static quenching is due to the formation of ground-state complex between fluorophore and quencher. The static quenching constant will decrease with increasing temperature, because higher temperature will lower the stability of the complex. Dynamic quenching results from collision between fluorophore and quencher, as higher temperatures result in larger diffusion coefficients, so the reverse effect is observed [22–24].

To confirm the quenching mechanism, the fluorescence quenching data were analyzed according to the Stern-Volmer equation (1). The Stern-Volmer plots of different temperatures and the corresponding results were shown in Figure 3 and Table 1. The results showed that K_{SV} decreased with increasing temperature, and k_q were much greater than 2.0×10^{10} L·mol^{-1}·s^{-1}, indicating a static quenching mechanism between BSA and DIO [25]. The quenching constants K_{SV} were both increased in the presence of Co^{2+} or Zn^{2+}, indicating that the presence of Co^{2+} or Zn^{2+} increased the fluorescence quenching effect of DIO. Meanwhile, the k_q values in the presence of Co^{2+} or Zn^{2+} suggest a static quenching mechanism for the binding of DIO to BSA with Co^{2+} or Zn^{2+}.

In order to obtain the binding constants, the experimental data were also analyzed according to the modified Stern-Volmer equation (2). Figure 4 showed the modified Stern-Volmer plots at different temperatures, and the calculated binding constants K for BSA-DIO system were listed in Table 2. The K values for the binding of DIO with BSA were decreased with increasing temperature, which further suggested that the binding of DIO with BSA was static quenching. The binding constants K for BSA-DIO system in the presence of Co^{2+} or Zn^{2+} were calculated to be 2.10×10^5 L·mol^{-1} and 1.94×10^5 L·mol^{-1}, respectively. The binding constants K for BSA-DIO system were both increased in the presence of Co^{2+} or Zn^{2+}, implying stronger binding of DIO to BSA in the present of Co^{2+} or Zn^{2+}.

3.3. The Nature of the Binding Forces. Generally, small organic molecules bound to biomolecules mainly through four types of acting forces: hydrogen bond, van der Waals' force, electrostatic force, and hydrophobic interaction, and so forth [26]. The force type can be determined by three thermodynamic parameters, enthalpy (ΔH^0), free-energy change (ΔG^0), and the entropy change (ΔS^0). These parameters for the interaction between DIO and BSA were calculated by Van't Hoff equation (3) and thermodynamic equation (4). The Van't Hoff plots were shown in Figure 5, and the thermodynamic parameters were listed in Table 2. The negative ΔG^0 suggested that the reactions between DIO and BSA were spontaneous. DIO bound to BSA mainly through the hydrogen bond and Van der Waals' force as evidenced by the negative value of ΔH^0 and ΔS^0 [27].

3.4. Energy Transfer between Drugs and BSA. The overlap of the absorption spectrum of DIO and the fluorescence emission spectrum of BSA is shown in Figure 6. For BSA, $K^2 = 2/3$, $\Phi = 0.15$, and $n = 1.336$ [28]; then we can obtain the following results: $J = 8.36 \times 10^{-14}$ cm^3·L·mol^{-1}, $R_0 = 3.64$ nm, and $r = 5.36$ nm. The distance between BSA and DIO was smaller than 8 nm, which suggested that the quenching of BSA by DIO was static quenching, which was in accordance with the results above.

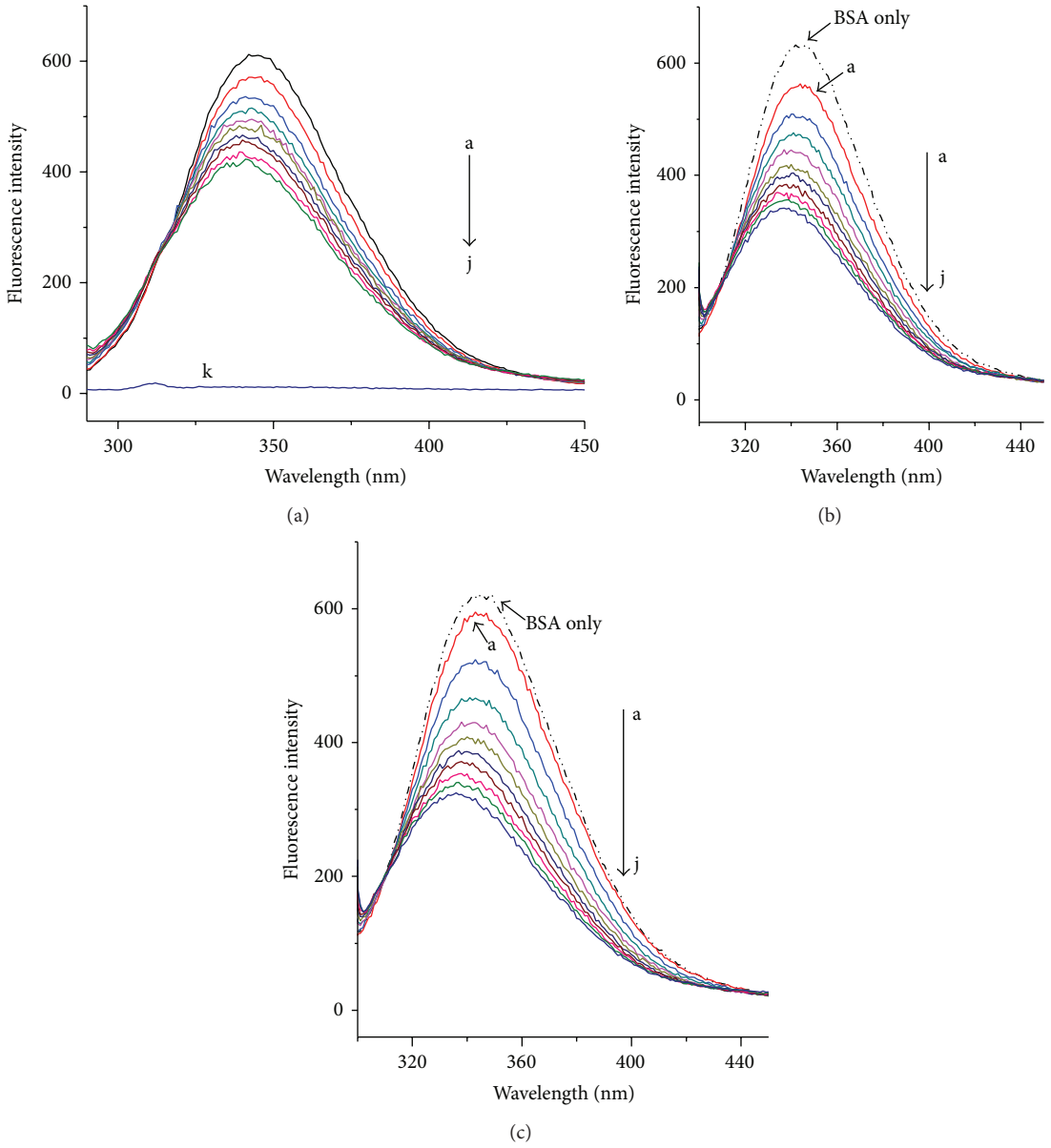

Figure 2: The fluorescence spectra of BSA by DIO in the absence and presence of Co^{2+} or Zn^{2+}. (a) BSA-DIO system; (b) BSA-DIO-Co^{2+} system; (c) BSA-DIO-Zn^{2+} system. From a to j, the concentration of DIO was varied from 0 to 9×10^{-6} mol·L^{-1} at increments of 1×10^{-6} mol·L^{-1}. k: DIO only, 9×10^{-6} mol·L^{-1}. [BSA] = [Co^{2+}] = [Zn^{2+}] = 5×10^{-7} mol·L^{-1}, T = 298 K.

Table 1: The Stern-Volmer quenching constants of DIO with BSA.

	T (K)	K_{SV} ($\times 10^4$·mol^{-1})	k_q ($\times 10^{12}$ L·mol^{-1}·s^{-1})	R^a	S.D.[b]
DIO-BSA	291	7.47	7.47	0.9928	0.03
	298	5.23	5.23	0.9947	0.02
	306	4.31	5.23	0.9964	0.01
BSA-DIO-Co^{2+}	298	7.83	4.31	0.9958	0.02
BSA-DIO-Zn^{2+}	298	9.58	7.83	0.9923	0.04

[a] R is the correlation coefficient; [b] S.D. is the standard deviation for the K_{SV} values.

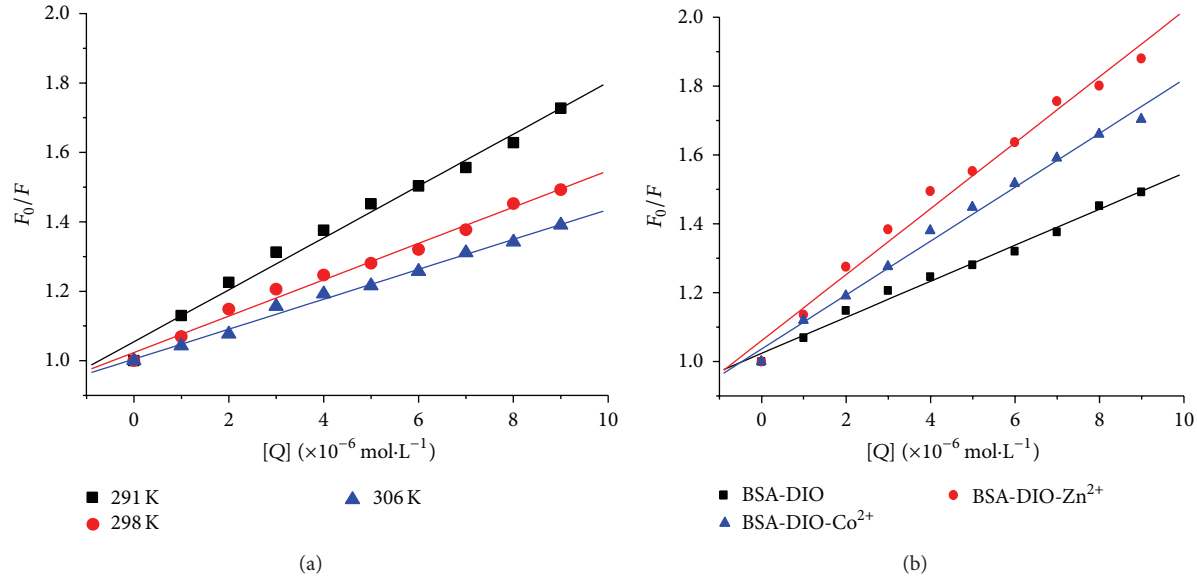

Figure 3: The Stern-Volmer plots for the binding of DIO with BSA at different temperatures (a) and in the absence and presence of Co^{2+} or Zn^{2+}, T = 298 K (b).

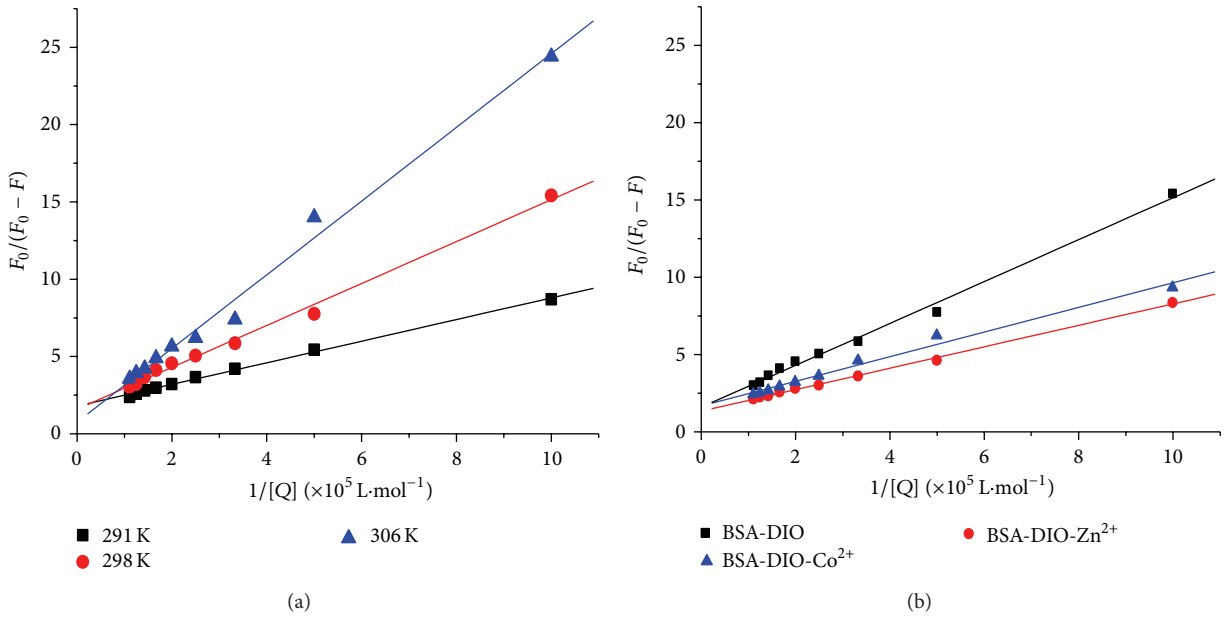

Figure 4: The modified Stern-Volmer plots for the binding of DIO with BSA at different temperatures (a) and in the absence and presence of Co^{2+} or Zn^{2+}, T = 298 K (b).

Table 2: The static binding constants K and thermodynamic parameters of DIO with BSA at different temperatures.

	T (K)	K ($\times 10^5$ L·mol^{-1})	R^a	ΔG^0 (kJ·mol^{-1})	ΔS^0 (J·mol^{-1}·K^{-1})	ΔH^0 (kJ·mol^{-1})
DIO-BSA	291	2.57	0.9985	−30.31	−252.48	−103.78
	298	1.17	0.9971	−28.54		
	306	0.32	0.9948	−26.52		

[a] R is the correlation coefficient for the K values.

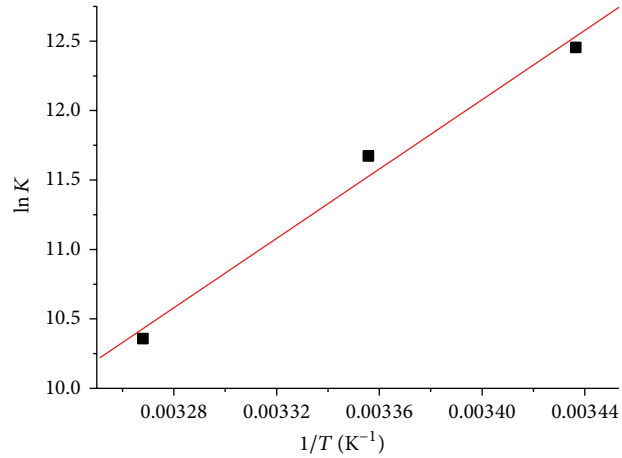

Figure 5: Van't Hoff plots for the binding of DIO with BSA.

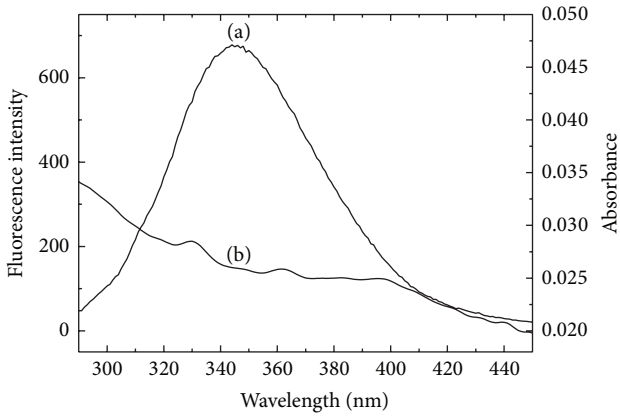

Figure 6: Spectral overlap between the fluorescence emission spectrum of BSA and the absorption spectrum of DIO. (a) fluorescence emission spectrum of BSA (5.0×10^{-7} mol·L^{-1}); (b) absorption spectrum of DIO (5.0×10^{-7} mol·L^{-1}).

3.5. The Binding of Site Maker Probes. There were two major binding sites for drugs on albumin which were known as Sudlow sites I and II. Site I is formed as a pocket in subdomain IIA and involves the lone tryptophan of the protein (^{212}Trp). Site I is adaptable and binds kinds of ligands with very different chemical structures. Site II locate at subdomain IIIA. It can bind smaller ligands because it is smaller, less flexible, and narrower than site I [29, 30]. Site I showed affinity for warfarin, ketoprofen, and so forth, and site II for ibuprofen, flufenamic acid, and so forth [31–33]. In order to determine the binding sites of DIO to BSA, the competitive displacement experiments were carried out using different site probes of ketoprofen for site I and ibuprofen for site II, respectively. The results showed that the binding constants of DIO to BSA were surprisingly changed from 2.57 to 1.304×10^5 L·mol^{-1} in the presence of ketoprofen, while the K values almost remained the same in the case of ibuprofen (2.47×10^5 L·mol^{-1}). The results indicated that ketoprofen exhibited

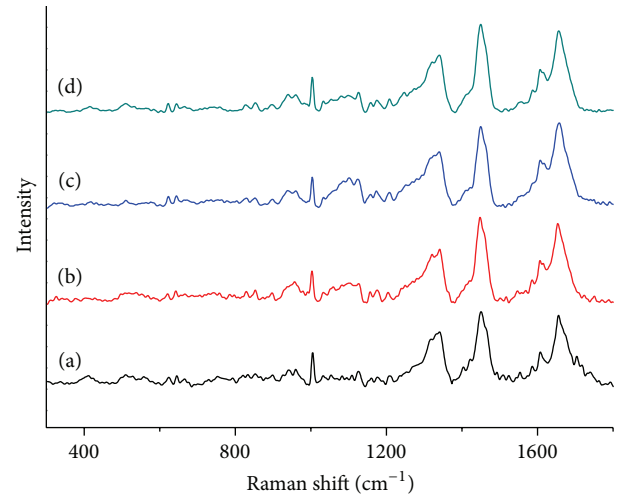

Figure 7: Raman spectra of (a) free BSA; (b) DIO-BSA system; (c) DIO-BSA-Co^{2+} system; (d) DIO-BSA-Zn^{2+} system. [BSA] = [DIO] = [Co^{2+}] = [Zn^{2+}] = 5×10^{-4} mol·L^{-1}.

significant displacement of DIO. However, ibuprofen was not displaced by DIO obviously. These meant that the binding site of DIO to BSA was site I.

3.6. Analysis of BSA Conformational Changes. Raman spectroscopy has emerged as a useful method to investigate the conformational changes of protein secondary structure and the microenvironment of amino acid residues [34]. In order to study the effects of DIO on the conformation of BSA, we analyzed the amide I and the regions of aromatic amino acid residues of Raman spectra. In Raman spectra, the peaks that appeared in the region of 1550–1620 cm^{-1} were the ring vibration bands of aromatic residues [35]. The amide I band (1700–1630 cm^{-1}) originated mainly from peptide C=O stretching [36, 37]. Figure 7 displayed the Raman spectra of BSA and BSA-DIO system in the absence and presence of Co^{2+} and Zn^{2+}. In the amide I band of BSA, the major band of BSA around 1648–1658 cm^{-1} was the characterization of α-helix; while the band of 1630–1640 cm^{-1} represented short segment chains connecting the α-helix, the bands of β-turn were centered at 1680–1700 cm^{-1}, respectively [38–42]. Figure 8 was the curve fitting of Raman amide I; the corresponding results were listed in Table 3. The results showed that native BSA contains major α-helix conformation (55.71%), which are consistent with the previous ones reported for BSA by Raman, infrared, and CD spectroscopy [43–45]. The α-helix contents decreased to 47.58% due to the binding of DIO. Meanwhile, the content of β-turn increased while the content of short segment decreased. The results indicated that the secondary structure of BSA was changed by DIO. Competing with the BSA-DIO system, the decreased extent of α-helix content was lower in the presence of Zn^{2+}, while for Co^{2+} there was an increase. The results indicated that the presence of Co^{2+} or Zn^{2+} affects the changes of BSA secondary structure.

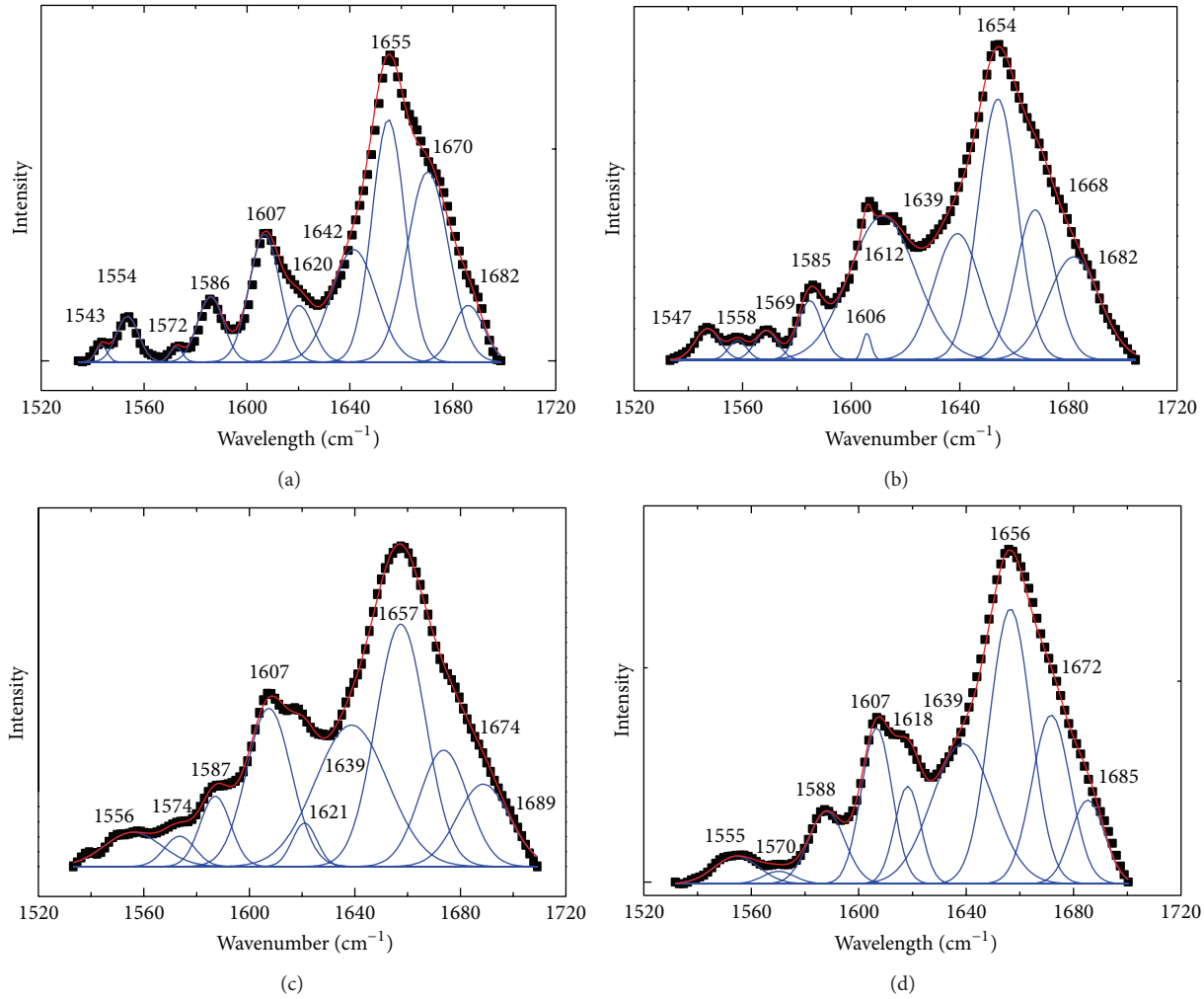

FIGURE 8: The curve fitting of Raman amide I of (a) free BSA; (b) DIO-BSA system; (c) DIO-BSA-Co^{2+} system; (d) DIO-BSA-Zn^{2+} system. The experimental spectra (black dots); the fitting curves (solid line).

TABLE 3: The curve fitting results of Raman amide *I* of BSA.

System		α-Helix	Short segment	β-Turn
BSA	Frequency (cm^{-1})	1655	1642	1682
	Content (%)	55.71	34.51	9.78
BSA-DIO	Frequency (cm^{-1})	1654	1639	1682
	Content (%)	47.58	27.70	24.72
BSA-DIO-Co^{2+}	Frequency (cm^{-1})	1657	1639	1689
	Content (%)	45.55	38.52	15.93
BSA-DIO-Zn^{2+}	Frequency (cm^{-1})	1657	1639	1685
	Content (%)	51.48	38.30	10.22

The conformation of 17 disulphide bridges of serum albumin molecule can be sensitively determined by Raman spectroscopy. The disulphide bridges of BSA have three conformations: gauche-gauche-gauche (g-g-g, peaks around 510 cm^{-1}), gauche-gauche-trans or trans-gauche-gauche (g-g-t or t-g-g, peaks around 525 cm^{-1}), and trans-gauche-trans (t-g-t, peaks around 540 cm^{-1}) [46]. Figure 9 was the analysis of the S-S bands; the conformations of 17 disulphide bridges were obtained according to the fitting results. As shown in Table 4, the major conformation of disulphide bridges in native BSA was g-g-g conformations. After binding DIO, there were 7 S-S bridges converted conformations, while 3

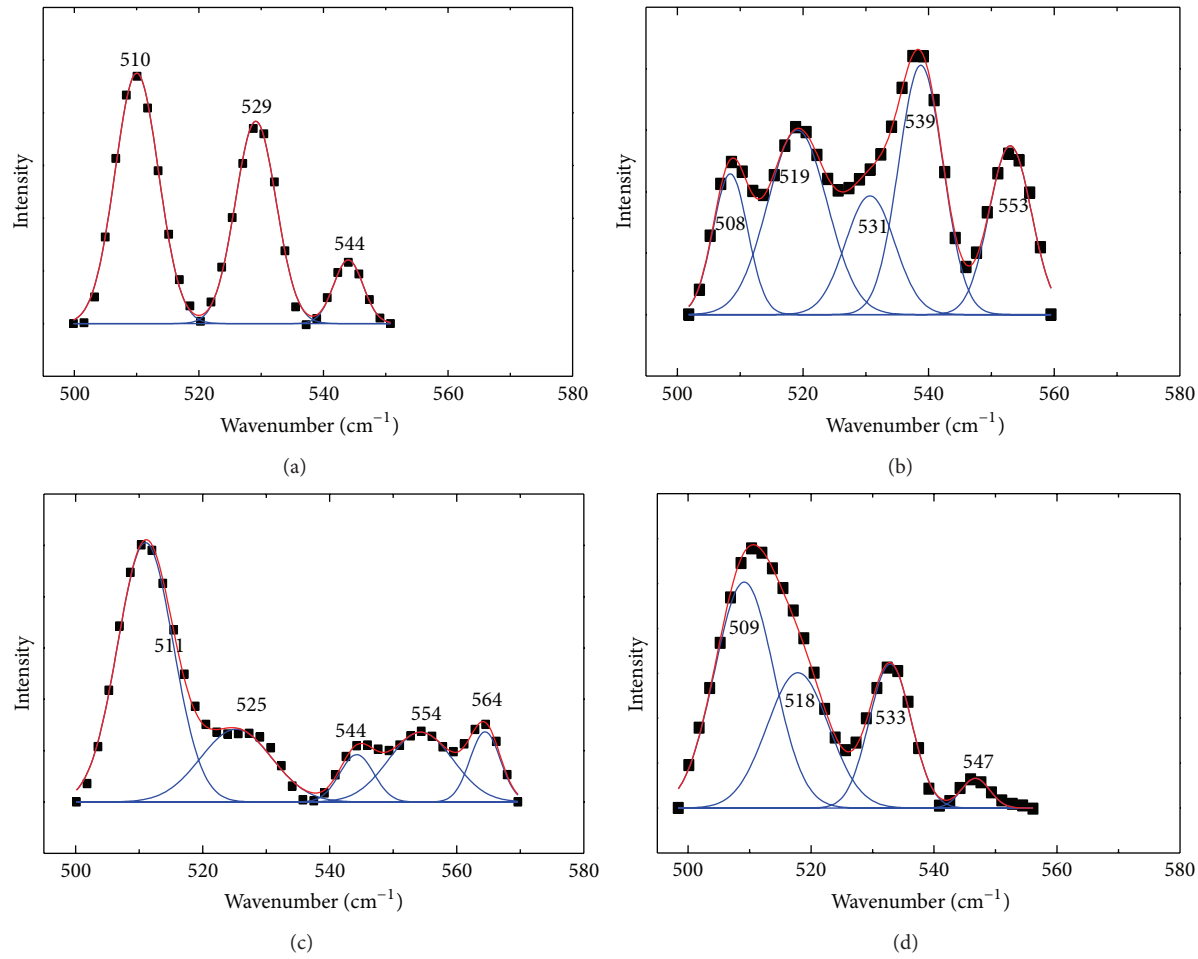

Figure 9: The analysis of the S-S bands of (a) free BSA; (b) DIO-BSA system; (c) DIO-BSA-Co^{2+} system; (d) DIO-BSA-Zn^{2+} system. The experimental spectra (black dots), the fitting curves (solid line).

Table 4: The conformation of the 17 disulfide bridges of BSA.

System	g-g-g	g-g-t or t-g-g	t-g-t	change
BSA	9	7	1	—
BSA-DIO	2	9	6	7
BSA-DIO-Co^{2+}	12	4	1	3
BSA-DIO-Zn^{2+}	8	5	4	3

Table 5: The analysis of the Tyr and Trp side chains.

System	BSA	BSA-DIO	BSA-DIO-Co^{2+}	BSA-DIO-Zn^{2+}
I_{850}/I_{830}	1.7180	1.0352	2.1477	2.1645
I_{1363}/I_{1340}	0.0409	0.0461	0.0502	0.0574

conformations of S-S bridges were changed in the presence of Co^{2+} or Zn^{2+}, which indicated the presence of Co^{2+} or Zn^{2+} decreased the changed of DIO to S-S bridges.

The tyrosyl doublet around 850 and 830 cm^{-1}, so-called "Fermi-resonance Tyr-doublet, was due to the symmetric ring-breathing vibration and the out-of-plane ring-bending vibration. The bands at 850 and 830 cm^{-1} are extremely sensitive to hydrogen bonding of the phenolic OH-groups, and the intensity ratio of this doublet (I_{850}/I_{830}) is an indicator of the microenvironment of tyrosine residues. The value of this ratio between 0.3 and 0.5 indicated that the tyrosyl residues were "buried." On the other hand, the tyrosine residues were "exposed," when the values range from 1.25 to 1.40 [47, 48]. The analysis of the Tyr side chains was displayed in Figure 10; the results in Table 5 showed that the value of I_{850}/I_{830} decreased after the addition of DIO. But I_{850}/I_{830} for BSA-DIO-Co^{2+} and BSA-DIO-Zn^{2+} systems were both increased in the presence of Co^{2+} or Zn^{2+}, and the values were larger than that of free BSA. The results indicated that the buriedness of Tyr residues in protein was increased by DIO, but the presence of Co^{2+} or Zn^{2+} decreased the buriedness of Tyr residues [49].

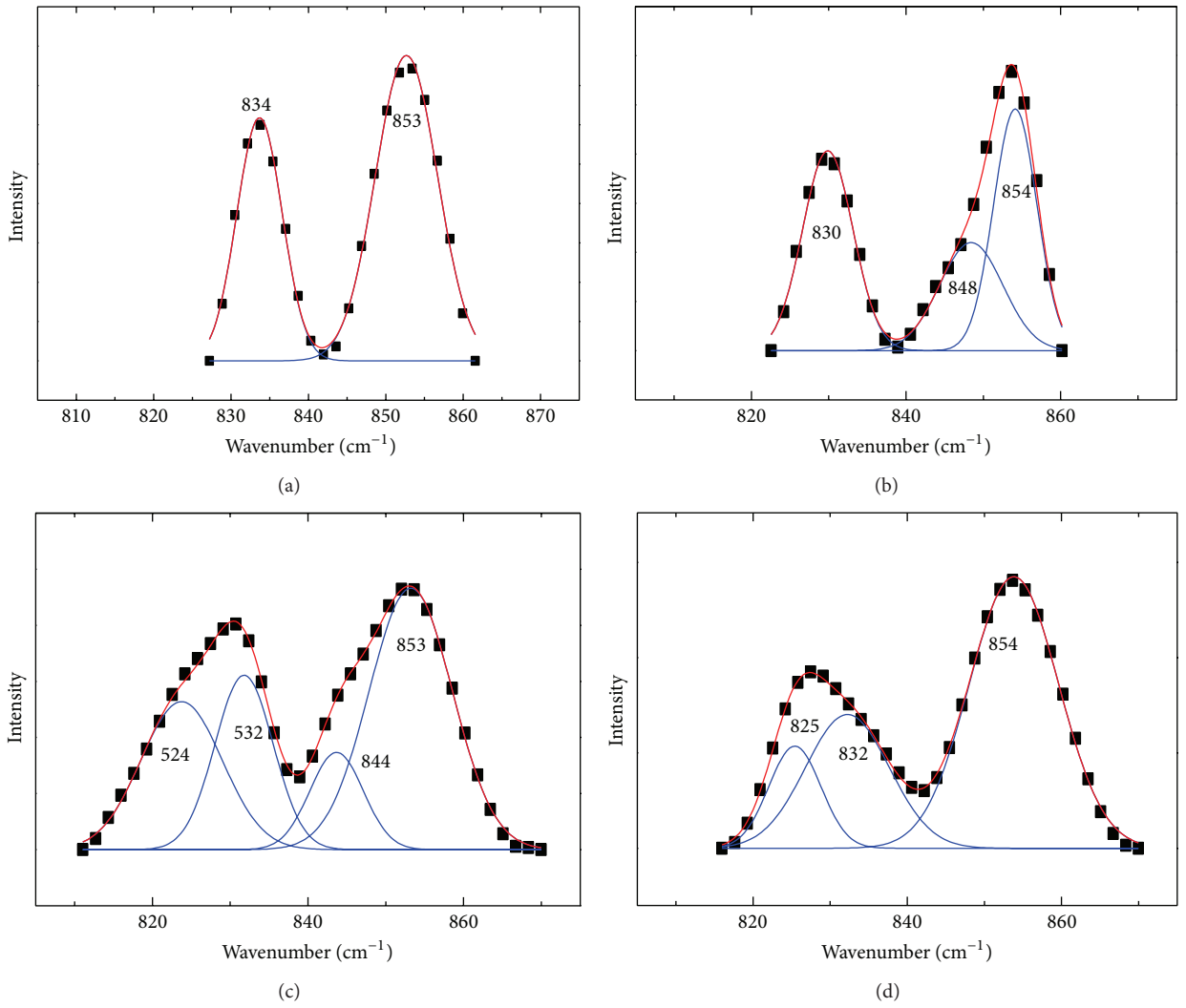

FIGURE 10: The analysis of the Tyr side chains of (a) free BSA; (b) DIO-BSA system; (c) DIO-BSA-Co^{2+} system; (d) DIO-BSA-Zn^{2+} system. The experimental spectra (black dots), the fitting curves (solid line).

The band appeared around 1340 cm^{-1} and the weak shoulder around 1363 cm^{-1} owing to the Fermi-resonance doublet bands of Trp residues. Their intensity ratio I_{1363}/I_{1340} can also be used to investigate the overall hydrophobicity of the environment surrounding tryptophan residues [50, 51]. Figure 11 was the analysis of the Trp side chains; the results were listed in Table 5. The intensity ratio of I_{1363}/I_{1340} increased from 0.0409 to 0.0461 due to the addition of DIO, while greater changes were found in BSA-DIO-Co^{2+} and BSA-DIO-Zn^{2+} systems. The results indicated that the hydrophobicity around the Trp residues increased due to the binding of DIO; the hydrophobicity increased more in the presence of Co^{2+} and Zn^{2+} [51].

4. Conclusions

In summary, we simulated the interaction of DIO with BSA in vitro by spectroscopic investigations. The experimental results indicated that the drugs could bind with BSA to form a DIO-BSA complex. The binding reaction was spontaneous. DIO bound to site I of BSA mainly through the hydrogen bond and Van der Waals' force. The presence of Co^{2+} or Zn^{2+} increased the quenching effect and the binding affinity of DIO to BSA. Otherwise, the analysis of conformation change confirmed that the binding of DIO induced the unfolding of protein secondary structure. Although the changes of BSA secondary structure caused by DIO in the presence of Co^{2+} or Zn^{2+} were different from those without metal ions, they all major led to the decrease of α-helix conformation. The addition of DIO changed 7 conformations of S-S bridges of BSA, while the changes were both reduced to 3 in the presence of Co^{2+} or Zn^{2+}. Besides, DIO increased the buriedness of Tyr residues in protein, but the effects were opposite for BSA-DIO-Co^{2+} and BSA-DIO-Zn^{2+} systems. Meanwhile, the hydrophobicity around the tryptophan residues was all increased due to the binding of DIO in the absence and presence of Co^{2+} or Zn^{2+}.

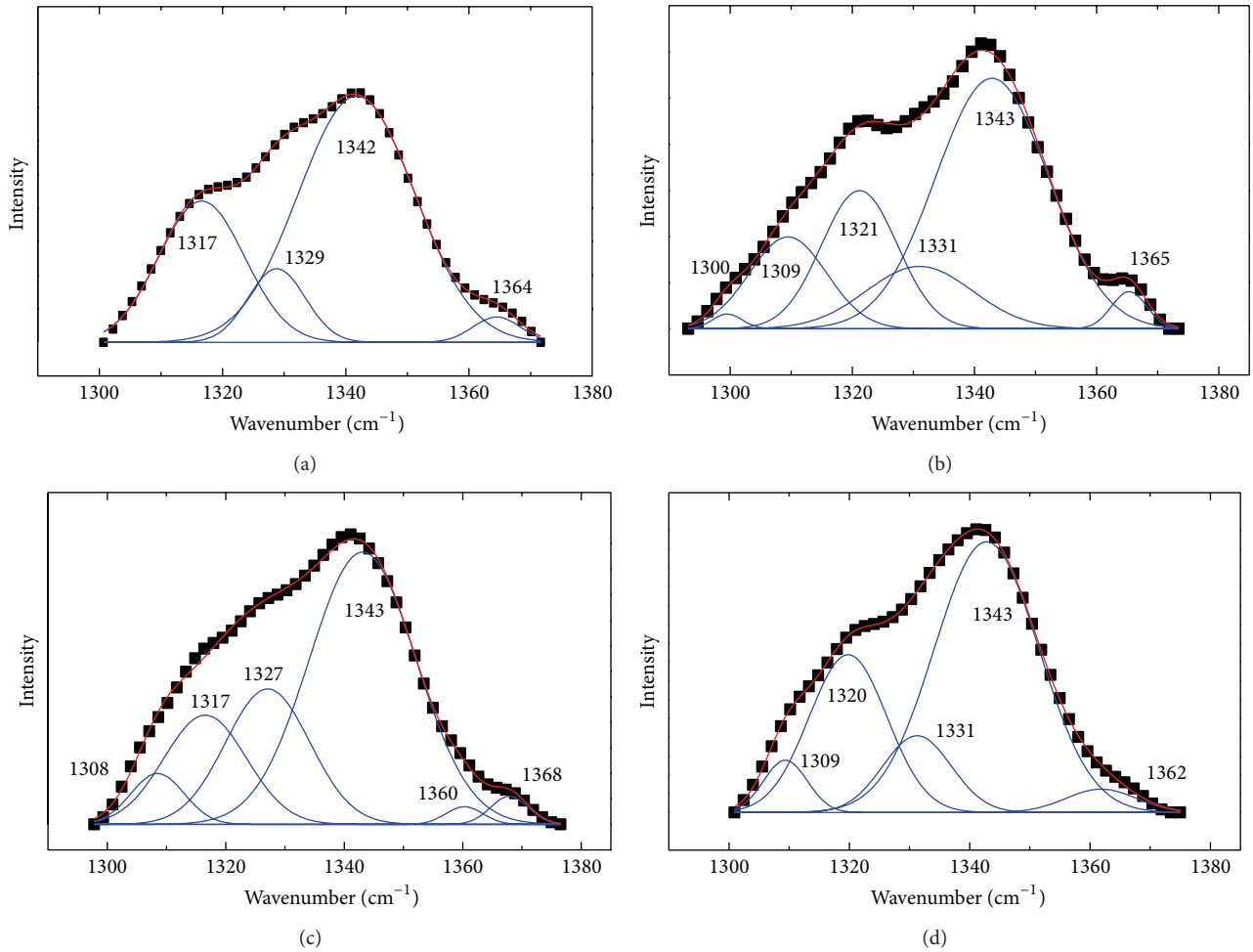

FIGURE 11: The analysis of the Trp side chains of (a) free BSA; (b) DIO-BSA system; (c) DIO-BSA-Co^{2+} system; (d) DIO-BSA-Zn^{2+} system. The experimental spectra (black dots), the fitting curves (solid line).

Conflict of Interests

The authors declare that there is no conflict of interests regarding the publication of this paper.

Acknowledgments

The authors gratefully acknowledge the National Natural Science Foundation of China (21061002, 21361003, and 21101035), the Scientific Research Foundation for the Returned overseas Chinese Scholars, the Guangxi Natural Science Foundation of China (2011GXNSFC018009, 2012GXNSFAA053035), Talent's Small Highland project of Guangxi Medicinal Industry (1201), and the Foundation of Key Laboratory for Chemistry and Molecular Engineering of Medicinal Resources.

References

[1] K. Higdon, A. Scott, M. Tucci et al., "The use of estrogen, dhea, and diosgenin in a sustained delivery setting as a novel treatment approach for osteoporosis in the ovariectomized adult rat model," *Biomedical Sciences Instrumentation*, vol. 37, pp. 281–286, 2001.

[2] R. E. Temel, J. M. Brown, Y. Ma et al., "Diosgenin stimulation of fecal cholesterol excretion in mice is not NPC1L1 dependent," *Journal of Lipid Research*, vol. 50, no. 5, pp. 915–923, 2009.

[3] T. Yamada, M. Hoshino, T. Hayakawa et al., "Dietary diosgenin attenuates subacute intestinal inflammation associated with indomethacin in rats," *The American Journal of Physiology: Gastrointestinal and Liver Physiology*, vol. 273, no. 2, pp. G355–G364, 1997.

[4] K. L. G. Dias, N. D. A. Correia, K. K. G. Pereira et al., "Mechanisms involved in the vasodilator effect induced by diosgenin in rat superior mesenteric artery," *European Journal of Pharmacology*, vol. 574, no. 2-3, pp. 172–178, 2007.

[5] Z. Yu, D. Li, B. Ji, and J. Chen, "Characterization of the binding of nevadensin to bovine serum albumin by optical spectroscopic technique," *Journal of Molecular Structure*, vol. 889, no. 1–3, pp. 422–428, 2008.

[6] U. R. Chatterjee, S. Ray, V. Micard et al., "Interaction with bovine serum albumin of an anti-oxidative pectic arabinogalactan from *Andrographis paniculata*," *Carbohydrate Polymers*, vol. 101, pp. 342–348, 2014.

[7] X. Xu, L. Zhang, D. Shen, H. Wu, and Q. Liu, "Oxygen-dependent oxidation of Fe(II) to Fe(III) and interaction of Fe(III) with bovine serum albumin, leading to a hysteretic effect on the fluorescence of bovine serum albumin," *Journal of Fluorescence*, vol. 18, no. 1, pp. 193–201, 2008.

[8] H. Liang, B. Xin, X. Wang, Y. Yuan, Y. Zhou, and P. Shen, "Equilibrium dialysis study on the interaction between Cu(II) and HSA or BSA," *Chinese Science Bulletin*, vol. 43, no. 5, pp. 404–409, 1998.

[9] H. Liang, J. Huang, C.-Q. Tu, M. Zhang, Y.-Q. Zhou, and P.-W. Shen, "The subsequent effect of interaction between Co^{2+} and human serum albumin or bovine serum albumin," *Journal of Inorganic Biochemistry*, vol. 85, no. 2-3, pp. 167–171, 2001.

[10] S. M. T. Shaikh, J. Seetharamappa, P. B. Kandagal, and D. H. Manjunatha, "Antioxidant Chinese yam polysaccharides and its pro-proliferative effect on endometrial epithelial cells," *International Journal of Biological Macromolecules*, vol. 41, no. 1, pp. 81–86, 2007.

[11] P. N. Naik, S. A. Chimatadar, and S. T. Nandibewoor, "Interaction between a potent corticosteroid drug—dexamethasone with bovine serum albumin and human serum albumin: a fluorescence quenching and fourier transformation infrared spectroscopy study," *Journal of Photochemistry and Photobiology B: Biology*, vol. 100, no. 3, pp. 147–159, 2010.

[12] Y. Q. Wang, H. M. Zhang, G. C. Zhang, W. H. Tao, and S. H. Tang, "Binding of rare earth metal complexes with an ofloxacin derivative to bovine serum albumin and its effect on the conformation of protein," *Journal of Luminescence*, vol. 126, pp. 211–218, 2007.

[13] Y. Ni, G. Liu, and S. Kokot, "Fluorescence spectrometric study on the interactions of isoprocarb and sodium 2-isopropylphenate with bovine serum albumin," *Talanta*, vol. 76, no. 3, pp. 513–521, 2008.

[14] S. S. Lehrer, "Solute perturbation of protein fluorescence. The quenching of the tryptophyl fluorescence of model compounds and of lysozyme by iodide ion," *Biochemistry*, vol. 10, no. 17, pp. 3254–3263, 1971.

[15] W. He, Y. Li, C. Xue, Z. Hu, X. Chen, and F. Sheng, "Effect of Chinese medicine alpinetin on the structure of human serum albumin," *Bioorganic and Medicinal Chemistry*, vol. 13, no. 5, pp. 1837–1845, 2005.

[16] T. Förster and O. Sinanoglu, *Modern Quantum Chemistry*, Academic Press, New York, NY,USA, 1966.

[17] J. R. Lakowicz, *Principles of Fluorescence Spectroscopy*, Plenum Press, New York, NY, USA, 1983.

[18] W. D. Horrocks Jr. and A. Peter Snyder, "Measurement of distance between fluorescent amino acid residues and metal ion binding sites. Quantitation of energy transfer between tryptophan and terbium(III) or europium(III) in thermolysin," *Biochemical and Biophysical Research Communications*, vol. 100, no. 1, pp. 111–117, 1981.

[19] P. B. Kandagal, J. Seetharamappa, S. Ashoka, S. M. T. Shaikh, and D. H. Manjunatha, "Study of the interaction between doxepin hydrochloride and bovine serum albumin by spectroscopic techniques," *International Journal of Biological Macromolecules*, vol. 39, no. 4-5, pp. 234–239, 2006.

[20] A. Sułkowska, M. Maciazek-Jurczyk, B. Bojko et al., "Competitive binding of phenylbutazone and colchicine to serum albumin in multidrug therapy: a spectroscopic study," *Journal of Molecular Structure*, vol. 881, no. 1–3, pp. 97–106, 2008.

[21] T. Yuan, A. M. Weljie, and H. J. Vogel, "Tryptophan fluorescence quenching by methionine and selenomethionine residues of calmodulin: orientation of peptide and protein binding," *Biochemistry*, vol. 37, no. 9, pp. 3187–3195, 1998.

[22] D. Ran, X. Wu, J. Zheng et al., "Study on the interaction between florasulam and bovine serum albumin," *Journal of Fluorescence*, vol. 17, no. 6, pp. 721–726, 2007.

[23] M. Xu, F.-J. Chen, L. Huang, P.-X. Xi, and Z.-Z. Zeng, "Binding of rare earth metal complexes with an ofloxacin derivative to bovine serum albumin and its effect on the conformation of protein," *Journal of Luminescence*, vol. 131, no. 8, pp. 1557–1565, 2011.

[24] J. R. Lakowicz, *Principles of Fluorescence Spectroscopy*, Kluwer Academic/Plenum, New York, NY, USA, 2nd edition, 1999.

[25] P. Banerjee, S. Pramanik, A. Sarkar, and S. C. Bhattacharya, "Deciphering the fluorescence resonance energy transfer signature of 3-pyrazolyl 2-pyrazoline in transport proteinous environment," *The Journal of Physical Chemistry B*, vol. 113, no. 33, pp. 11429–11436, 2009.

[26] S. N. Timaseff, "Thermodynamics of protein interactions," in *Proteins of Biological Fluids*, H. Peeters, Ed., pp. 511–519, Pergamon Press, Oxford, UK, 1972.

[27] P. D. Ross and S. Subramanian, "Thermodynamics of protein association reactions: forces contributing to stability," *Biochemistry*, vol. 20, no. 11, pp. 3096–3102, 1981.

[28] X.-Z. Feng, Z. Lin, L.-J. Yang, C. Wang, and C.-L. Bai, "Investigation of the interaction between acridine orange and bovine serum albumin," *Talanta*, vol. 47, no. 5, pp. 1223–1229, 1998.

[29] T. Peters, *All about Albumin: Biochemistry, Genetics, and Medical Applications*, Academic Press, San Diego, CA, USA, 1996.

[30] U. Krach-Hansen, V. T. G. Chuang, and M. Otagiri, "Practical aspects of the ligand-binding and enzymatic properties of human serum albumin," *Biological and Pharmaceutical Bulletin*, vol. 25, no. 6, pp. 695–704, 2002.

[31] C. E. Petersen, C.-E. Ha, S. Curry, and N. V. Bhagavan, "Probing the structure of the warfarin-binding site on human serum albumin using site-directed mutagenesis," *Proteins: Structure, Function and Genetics*, vol. 47, no. 2, pp. 116–125, 2002.

[32] X. M. He and D. C. Carter, "Atomic structure and chemistry of human serum albumin," *Nature*, vol. 358, no. 6383, pp. 209–215, 1992.

[33] H. Greige-Gerges, R. A. Khalil, E. A. Mansour, J. Magdalou, R. Chahine, and N. Ouaini, "Cucurbitacins from *Ecballium elaterium* juice increase the binding of bilirubin and ibuprofen to albumin in human plasma," *Chemico-Biological Interactions*, vol. 169, no. 1, pp. 53–62, 2007.

[34] A. Misiunas, Z. Talaikyte, G. Niaura, V. Razumas, and T. Nylander, "Thermomyces lanuginosus lipase in the liquid-crystalline phases of aqueous phytantriol: X-ray diffraction and vibrational spectroscopic studies," *Biophysical Chemistry*, vol. 134, no. 3, pp. 144–156, 2008.

[35] C. David, S. Foley, C. Mavon, and M. Enescu, "Reductive unfolding of serum albumins uncovered by Raman spectroscopy," *Biopolymers*, vol. 89, no. 7, pp. 623–634, 2008.

[36] W. K. Surewicz, H. H. Mantsch, and D. Chapman, "Determination of protein secondary structure by fourier transform infrared spectroscopy: a critical assessment," *Biochemistry*, vol. 32, no. 2, pp. 389–394, 1993.

[37] A. I. Ivanov, E. A. Korolenko, E. V. Korolik et al., "Chronic liver and renal diseases differently affect structure of human serum albumin," *Archives of Biochemistry and Biophysics*, vol. 408, no. 1, pp. 69–77, 2002.

[38] J. T. Pelton and L. R. McLean, "Spectroscopic methods for analysis of protein secondary structure," *Analytical Biochemistry*, vol. 277, no. 2, pp. 167–176, 2000.

[39] B. M. Smith and S. Franzen, "Single-pass attenuated total reflection fourier transform infrared spectroscopy for the analysis of proteins in H_2O solution," *Analytical Chemistry*, vol. 74, no. 16, pp. 4076–4080, 2002.

[40] J. Fontecha, J. Bellanato, and M. Juarez, "Infrared and Raman spectroscopic study of casein in cheese: effect of freezing and frozen storage," *Journal of Dairy Science*, vol. 76, no. 11, pp. 3303–3309, 1993.

[41] H. Fabian and P. Anzenbacher, "New developments in Raman spectroscopy of biological systems," *Vibrational Spectroscopy*, vol. 4, no. 2, pp. 125–148, 1993.

[42] J. Wang, S. Li, X. L. Peng et al., "Multi-spectroscopic studies on the interaction of human serum albumin with astilbin: binding characteristics and structural analysis," *Journal of Luminescence*, vol. 136, pp. 422–429, 2013.

[43] Q. Yang, J. Liang, and H. Han, "Probing the interaction of magnetic iron oxide nanoparticles with bovine serum albumin by spectroscopic techniques," *The Journal of Physical Chemistry B*, vol. 113, no. 30, pp. 10454–10458, 2009.

[44] B. I. Baello, P. Pancoska, and T. A. Keiderling, "Enhanced prediction accuracy of protein secondary structure using hydrogen exchange fourier transform infrared spectroscopy," *Analytical Biochemistry*, vol. 280, no. 1, pp. 46–57, 2000.

[45] D. Li, M. Zhu, C. Xu, and B. Ji, "Characterization of the baicalein-bovine serum albumin complex without or with Cu^{2+} or Fe^{3+} by spectroscopic approaches," *European Journal of Medicinal Chemistry*, vol. 46, no. 2, pp. 588–599, 2011.

[46] H. E. Van Wart, A. Lewis, H. A. Scheraga, and F. D. Saeva, "Disulfide bond dihedral angles from Raman spectroscopy," *Proceedings of the National Academy of Sciences of the United States of America*, vol. 70, no. 9, pp. 2619–2623, 1973.

[47] Z. Jurasekova, G. Marconi, S. Sanchez-Cortes, and A. Torreggiani, "Spectroscopic and molecular modeling studies on the binding of the flavonoid luteolin and human serum albumin," *Biopolymers*, vol. 91, no. 11, pp. 917–927, 2009.

[48] P. R. Carey, *Biochemical Applications of Raman and Resonance Raman Spectroscopics*, Academic Press, New York, NY, USA, 1982.

[49] N.-T. Yu, B. H. Jo, and D. C. O'Shea, "Laser Raman scattering of cobramine B, a basic protein from cobra venom," *Archives of Biochemistry and Biophysics*, vol. 156, no. 1, pp. 71–76, 1973.

[50] T. Miura, H. Takeuchi, and I. Harada, "Characterization of individual tryptophan side chains in proteins using Raman spectroscopy and hydrogen-deuterium exchange kinetics," *Biochemistry*, vol. 27, no. 1, pp. 88–94, 1988.

[51] I. Harada, T. Miura, and H. Takeuchi, "Origin of the doublet at 1360 and 1340 cm^{-1} in the Raman spectra of tryptophan and related compounds," *Spectrochimica Acta A: Molecular Spectroscopy*, vol. 42, no. 2-3, pp. 307–312, 1986.